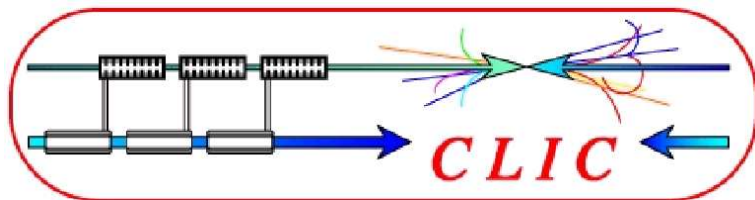


## CERN - EUROPEAN ORGANIZATION FOR NUCLEAR RESEARCH



CLIC Note 737

# DESIGN STUDY OF THE CLIC INJECTOR AND BOOSTER LINACS WITH THE 2007 BEAM PARAMETERS

A. Ferrari<sup>†</sup>, A. Latina<sup>\*</sup>, L. Rinolfi<sup>\*</sup>

<sup>†</sup> Uppsala University, Sweden

<sup>\*</sup> CERN, Geneva, Switzerland

## Abstract

This note presents new particle tracking studies in the CLIC Injector and Booster Linacs, which accelerate both electrons and positrons, respectively from 200 MeV to 2.42 GeV, prior to their injection into the pre-damping rings, and from 2.42 to 9 GeV, before their transport to the main accelerating linacs.

CERN-OPEN-2008-017  
09/05/2008



May 9, 2008

# 1 Introduction

The Compact Linear Collider (CLIC) study explores the feasibility of the Two-Beam Acceleration technology using high-frequency (12 GHz) traveling-wave structures at room temperature. At CLIC, the electron and positron main beams are produced in a common injection complex [1], see Figure 1. Downstream of the electron and positron sources, a single 2 GHz Injector Linac accelerates both beams from 200 MeV to 2.42 GeV. Then, a bending magnet separates the electrons and the positrons, before injection into their respective pre-damping rings. With polarized particles, the nominal ring energy must be chosen such that the spin tune is a half-integer, i.e.  $E_{dr} = (n+1/2) 0.440 \text{ GeV} = 2.42 \text{ GeV}$  in our case. After the damping rings, the electron and positron beams go successively through a first stage of bunch compression at 2 GHz, a common 4 GHz Booster Linac which accelerates the beams up to 9 GeV, long transfer lines and a second stage of bunch compression at 12 GHz, prior to their injection into the main linacs.

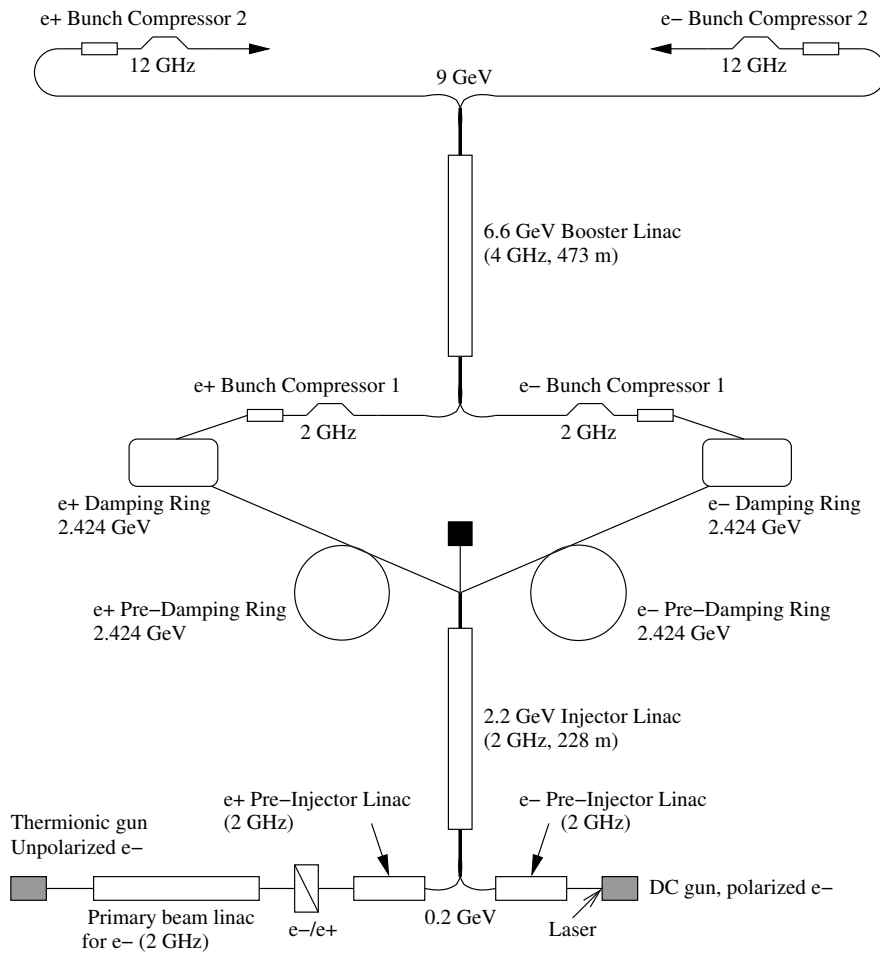


Figure 1: Layout of the CLIC injection complex, from the electron and positron sources to the entrance of the main linacs.

A first design of the Injector Linac was described in [2, 3]. In that study, transverse beam dynamics and particle tracking simulations were performed with MAD [4], with special emphasis on the positron beam, which has large transverse emittances. The proposed optics for the CLIC Injector Linac was then based on a FODO lattice wrapping the first six accelerating structures, followed by a succession of quadrupole triplets and accelerating structures for the rest of the linac. More recently, using PLACET [5] for particle tracking simulations, we showed that the short range wakefields do not affect the performance of the Injector Linac [6]. Since this study was published, a new set of CLIC beam parameters has been chosen. In particular, the accelerating gradient and the RF frequency in the main CLIC linac were lowered from 150 to 100 MV/m and from 30 to 12 GHz, respectively. This also affects the frequency and thereby the design of the accelerating structures in the injection complex. It is thus necessary to review the design of the CLIC Injector Linac, as well as to perform a more detailed study of the Booster Linac. In Section 2, a new design for the CLIC Injector Linac is presented and PLACET particle tracking studies are performed, in order to estimate the emittance growth in the linac and to determine the main properties of the beams prior to their injection into the damping rings. In Section 3, a first design of the CLIC Booster Linac is described, based on MAD simulations and PLACET particle tracking studies. Finally, some conclusions are given in Section 4.

## 2 Design study of the CLIC Injector Linac

The CLIC Injector Linac alternately accelerates electrons and positrons, from 200 MeV to 2.42 GeV. The main beam properties at the exit of the  $e^-$  and  $e^+$  Pre-Injector Linacs are given in Tables 1 and 2, respectively.

Table 1: Beam characteristics at the exit of the  $e^+$  Pre-Injector Linac [1].

Positron beam energy	200 MeV
Normalized emittance $\gamma\epsilon_{x/y}$	$9.2 \cdot 10^{-3}$ m.rad
Energy spread $\sigma_E$	7 MeV
Bunch length $\sigma_l$	5 mm
Bunch charge $Q$	1.1 nC

Table 2: Beam characteristics at the exit of the  $e^-$  Pre-Injector Linac [1].

Electron beam energy	200 MeV
Normalized emittance $\gamma\epsilon_{x/y}$	$10.0 \cdot 10^{-6}$ m.rad
Energy spread $\sigma_E$	2 MeV
Bunch length $\sigma_l$	1 mm
Bunch charge $Q$	0.8 nC

Following the change of the RF frequency in the main linac, as well as in the injection complex, a new design was considered for the accelerating structures of the CLIC Injector Linac. In our previous study, the electron and positron beams were brought from 200 MeV to 2.42 GeV by 26 accelerating structures operating at 1.5 GHz, with a length of 5 m and a loaded gradient of 17.1 MV/m each. For this new study of the CLIC Injector Linac, 37 accelerating structures operating at 2 GHz are used. Their length and loaded gradient are 4 m and 15 MV/m, respectively.

In the CLIC Injector Linac, one major constraint is to keep the transverse size of the positron beam as small as possible. A FODO lattice is therefore proposed for the first 15 accelerating structures at the beginning of the CLIC Injector Linac, until the energy is sufficiently high (and thus the geometrical emittance sufficiently small) to allow somewhat larger betatron functions inside the accelerating structures. In order to obtain maximal focusing while keeping a reasonable spacing between the quadrupoles, six 42 cm long quadrupoles are installed on each accelerating structure, with 24.7 cm between them. In addition, there is one doublet between each accelerating structure, where beam instrumentation can be inserted. The corresponding layout is shown in Figure 2.

For the rest of the Injector Linac, downstream of the 15th accelerating structure, another type of lattice is implemented, namely a succession of triplets and accelerating structures, as shown in Figure 3. In the triplet, the spacing between two consecutive quadrupoles, as well as between the edge of an accelerating structure and a quadrupole, is 30 cm.

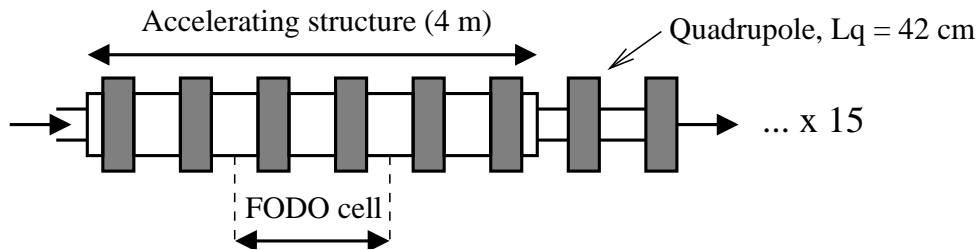


Figure 2: Layout of one of the 15 accelerating structures inside a FODO lattice, at the beginning of the Injector Linac.

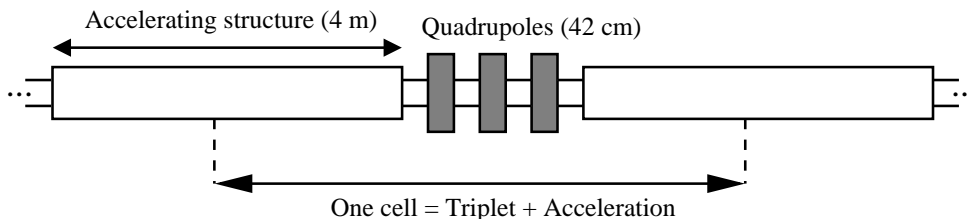


Figure 3: Layout of the Injector Linac downstream of the 15th accelerating structure.

## 2.1 Optics design and beam dynamics simulations with MAD

The betatron functions should be small, especially in the very first accelerating sections of the linac. This is generally achieved with a large focusing gradient in the quadrupoles of the FODO lattice, however the field strength should not exceed 1.2 T. If  $R_Q$  and  $K_Q$  are respectively the quadrupole aperture and normalized gradient, then one has:

$$K_Q = \frac{B/R_Q}{3.3356p [\text{GeV}/c]} \text{ and } B \leq 1.2 \text{ T} \implies R_Q [\text{m}] \leq \frac{0.36}{K_Q [\text{m}^{-2}] E_{out}^i [\text{GeV}]}, \quad (1)$$

where  $E_{out}^i$  is the energy at the exit of the accelerating structure  $i$  on which the quadrupole is installed.

Let us consider the first accelerating structure, for which the final energy is 260 MeV. In order to obtain a sufficiently small beam size ( $\beta \leq 2.5$  m) along the whole structure, one must set the normalized gradient  $K_Q$  to  $3.6 \text{ m}^{-2}$ , see Figure 4.

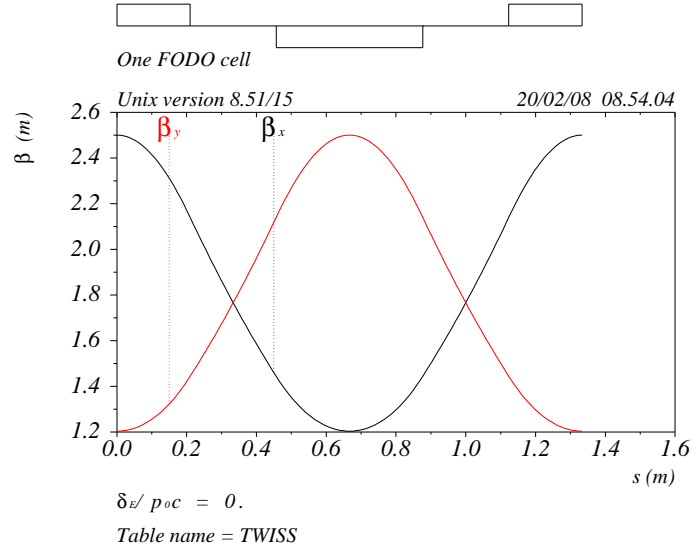


Figure 4: Betatron functions in one of (periodic) FODO cells at the very beginning of the CLIC Injector Linac.

Given the limitation on the pole-tip magnetic field, one must keep the quadrupole aperture below 38.4 cm in order to reach the desired focusing strength. If one applies the same condition to the 15th accelerating structure, then the largest acceptable value of  $R_Q$  becomes 9.1 cm (the energy is 1.1 GeV). It seems difficult to fit 2 GHz accelerating structures inside such a quadrupole. On the other hand, since the geometrical emittance is now about 4 times smaller than at the beginning of the FODO lattice, one can accept somewhat larger betatron functions. In turn, one may allow a smaller focusing strength for the quadrupole, which can be obtained by increasing its aperture.

As the beam energy increases, in order to have an adiabatic variation of the FODO lattice properties, we divide it into three sub-sections, with different periodic solutions:

- for the FODO cells wrapping the accelerating structures ACC1 to ACC5:  
 $K = \pm 3.60 \text{ m}^{-2} \Rightarrow 1.2 \text{ m} \leq \beta_{x,y} \leq 2.5 \text{ m}$ ,
- for the FODO cells wrapping the accelerating structures ACC6 to ACC10:  
 $K = \pm 2.50 \text{ m}^{-2} \Rightarrow 2.0 \text{ m} \leq \beta_{x,y} \leq 3.2 \text{ m}$ ,
- for the FODO cells wrapping the accelerating structures ACC11 to ACC15:  
 $K = \pm 1.88 \text{ m}^{-2} \Rightarrow 2.8 \text{ m} \leq \beta_{x,y} \leq 4.0 \text{ m}$ .

The layout of the FODO lattice must now include two matching sections, where the doublet consisting of a focusing quadrupole, a drift of 24.7 cm and a defocusing quadrupole is replaced by:

- between the 5th and 6th accelerating structures: a drift of 47.3 cm, a focusing quadrupole with  $K = +2.77 \text{ m}^{-2}$ , a drift of 62.1 cm, a defocusing quadrupole with  $K = -2.94 \text{ m}^{-2}$  and a drift of 30.8 cm,
- between the 10th and 11th accelerating structures: a drift of 85.9 cm, a focusing quadrupole with  $K = +1.98 \text{ m}^{-2}$ , a drift of 69.3 cm, a defocusing quadrupole with  $K = -2.38 \text{ m}^{-2}$  and a drift of 13.7 cm.

Figure 5 shows the betatron functions of the positron beam, as computed with the present optics, from the start of the CLIC Injector Linac to the exit of the 15th accelerating structure. The three sub-sections with different FODO cells and the two matching sections (at  $s \simeq 28 \text{ m}$  and  $s \simeq 56 \text{ m}$ ) are clearly visible. At the entrance of the linac,  $\beta_x = 1.44 \text{ m}$ ,  $\alpha_x = -1.20$  and  $\beta_y = 2.14 \text{ m}$ ,  $\alpha_y = +1.62$ .

In addition to the constraint of equation (1), one should take into account the positron beam sizes inside the 2 GHz accelerating structures. In order to transport more than 99% of the particles through the FODO lattice, the iris aperture must be exceed the largest rms transverse beam size for the positrons by at least a factor 3.

Using  $\sigma_{x,y} = \sqrt{\beta_{x,y} \times \epsilon_{x,y}}$ , this condition translates into:

$$R_{iris} [\text{m}] \geq 0.206 \sqrt{\frac{\beta_{max} [\text{m}]}{E_{in} [\text{MeV}]}} \quad (2)$$

where  $\beta_{max}$  and  $E_{in}$  are respectively the largest value of  $\beta_{x,y}$  along a given accelerating structure and the beam energy at its entrance.

Table 3 summarizes the constraints imposed on the 15 accelerating structures inside the FODO lattice, as derived from equations (1) and (2).

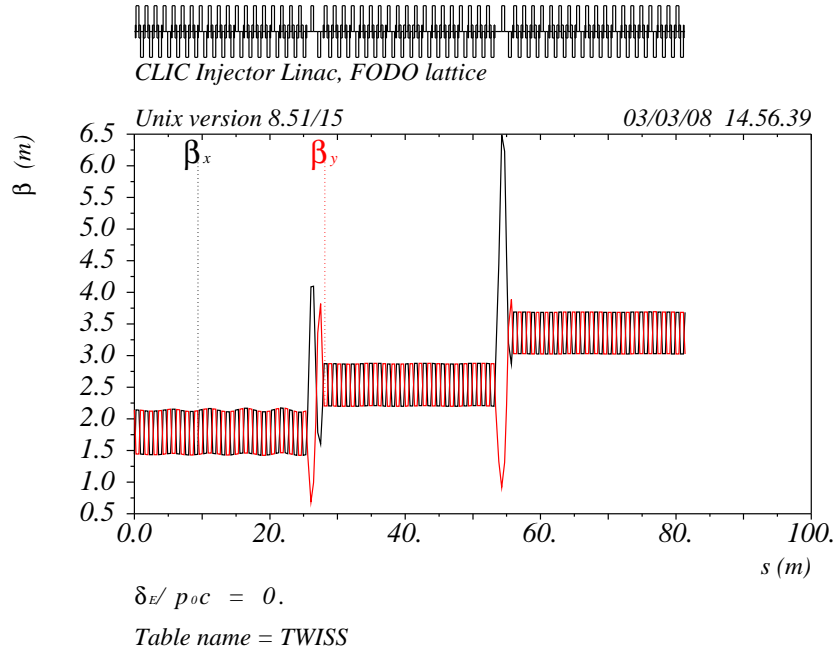


Figure 5: Betatron functions of the positron beam along the FODO lattice wrapping the 15 first accelerating structures of the CLIC Injector Linac.

Table 3: Constraints on the iris aperture and the external radius of the 15 accelerating structures inside the FODO lattice, at the beginning of the CLIC Injector Linac.

Structure number	1	2	3	4	5
Min( $R_{iris}$ ) in cm	2.30	2.01	1.82	1.67	1.55
Max( $R_Q$ ) in cm	38.4	31.2	26.3	22.7	20.0
Structure number	6	7	8	9	10
Min( $R_{iris}$ ) in cm	1.64	1.55	1.48	1.41	1.35
Max( $R_Q$ ) in cm	25.7	23.2	21.2	19.5	18.0
Structure number	11	12	13	14	15
Min( $R_{iris}$ ) in cm	1.45	1.40	1.35	1.31	1.28
Max( $R_Q$ ) in cm	22.3	20.9	19.6	18.5	17.4

A unique accelerating structure design, with an iris aperture of at least 2.5 cm (including about 2 mm for the vacuum pipe) and an external radius of at most 17.4 cm, is suitable for the whole FODO lattice section of the CLIC Injector Linac.

Let us now focus on the optics design in the section of the Injector Linac downstream of the 15th accelerating structure, where the periodic cell consists of a triplet and two half accelerating structures on either side. With  $K_e = +0.94 \text{ m}^{-2}$  for the outermost

quadrupoles of the triplet and  $K_m = -1.78 \text{ m}^{-2}$  for the quadrupole in the middle, both the horizontal and vertical betatron functions are equal to 6 m at the waist, located at the centre of the accelerating structure. In the middle of the second quadrupole (and thereby of the periodic cell),  $\beta_x$  and  $\beta_y$  are respectively 4.9 and 10.8 m, see Figure 6.

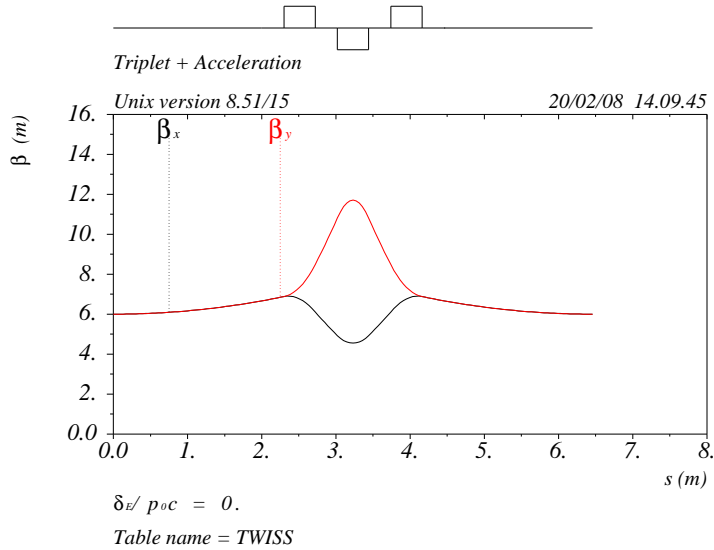


Figure 6: Betatron functions in a periodic cell with triplet + acceleration, located downstream of the 15th accelerating structure of the CLIC Injector Linac.

Note that, in contrary to the FODO lattice upstream, all quadrupoles now directly wrap the vacuum pipe, which allows to reach large focusing gradients in more relaxed conditions, since the aperture  $R_Q$  can be as small as a few cm. Indeed, the only significant technical constraint comes from the transverse beam size (especially in the vertical direction). In order to transport more than 99% of the particles from the 16th accelerating structure until the end of the Injector Linac, the vacuum pipe aperture must be exceed the largest rms transverse beam size for the positrons by at least a factor 3. With  $\beta_{max} = 10.8 \text{ m}$ , this condition translates into:

$$R_{pipe} [\text{m}] \geq \frac{0.676}{\sqrt{E [\text{MeV}]}}. \quad (3)$$

The most severe constraint is obtained at the exit of the 16th accelerating structure, where  $E = 1.16 \text{ GeV}$ : one must make sure that  $R_{pipe}$  remains larger than 2 cm, which is already satisfied if the iris of all accelerating structures is larger than 2.5 cm, as derived from Table 3.

Additional independent quadrupoles must be installed in front of the 16th accelerating structure, in order to match the betatron functions between the third FODO sub-section and the lattice with triplet + acceleration. The matching procedure in MAD is usually



straightforward and requires four independent quadrupoles only. However, subsequent tracking simulations along the whole CLIC Injector Linac suggest that an emittance increase of a few percent occur in the matching section. Indeed, the solution found by MAD for the reference particle can actually lead to a mismatch for particles with a somewhat lower or larger energy, and in turn to an emittance growth. Therefore, one should include not only the target Twiss parameters but also the desired values of the transverse emittances in the figure-of-merit function used in the matching procedure. Hence, six independent quadrupoles are needed in the matching section, see Figure 7. Like in the rest of the Injector Linac, these quadrupoles are 42 cm long. The distance between ACC15 and Q1, between Q6 and ACC16, as well as between two consecutive quadrupoles, is set to 1 m.

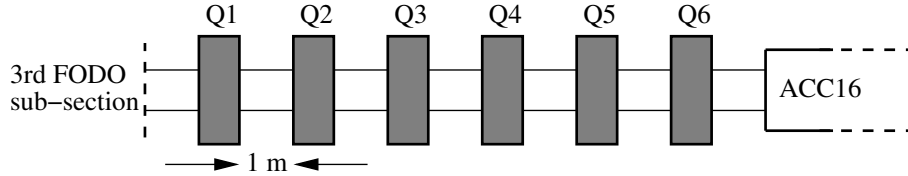


Figure 7: Layout of the matching section located between ACC15 and ACC16.

The matching is done using PLACET, in parallel with other tracking simulation studies. Indeed, the emittance growth at any location in the linac (e.g. in the matching section) strongly depends on the energy spread of the beam.

## 2.2 Particle tracking studies with PLACET

In the following, Gaussian distributions are used in order to describe the transverse and longitudinal phase spaces of the positron beam at the entrance of the linac (see Table 1). With on-crest acceleration, due to the non-zero bunch length, all positrons do not receive the maximum amount of energy when they pass through the accelerating structures, which may lead to additional energy spread. In turn, the positrons with a negative  $\delta p/p$  tend to be over-focused in the quadrupoles. These chromatic effects may eventually lead to an emittance growth.

The first step of our particle tracking studies is to minimize the emittance growth coming from the matching section between ACC15 and ACC16, while ensuring that the design values of the Twiss parameters are obtained for the positron beam at the end of the Injector Linac, namely  $\beta_x = \beta_y = 6.88$  m and  $\alpha_x = \alpha_y = -0.38$ . The result of this matching procedure is presented in Table 4.

Figures 8 and 9 show the evolution of the rms normalized emittances and of the betatron functions along the CLIC Injector Linac. These physical quantities are derived from the horizontal and vertical phase space distributions of the positron beam at several locations along the linac (a statistical approach is used for this purpose).

Table 4: Results of the matching procedure, when both the Twiss parameters and the transverse emittances obtained at the end of the CLIC Injector Linac are included in the figure-of-merit function.

Parameter	Value
$K_{Q1}$ in $\text{m}^{-2}$	+1.12
$K_{Q2}$ in $\text{m}^{-2}$	-0.98
$K_{Q3}$ in $\text{m}^{-2}$	+0.92
$K_{Q4}$ in $\text{m}^{-2}$	-1.39
$K_{Q5}$ in $\text{m}^{-2}$	+1.16
$K_{Q6}$ in $\text{m}^{-2}$	-0.47

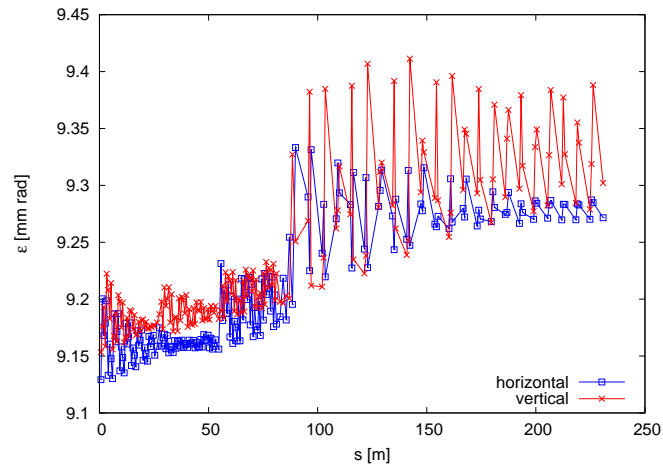


Figure 8: Transverse rms normalized emittances of the positron beam along the CLIC Injector Linac.

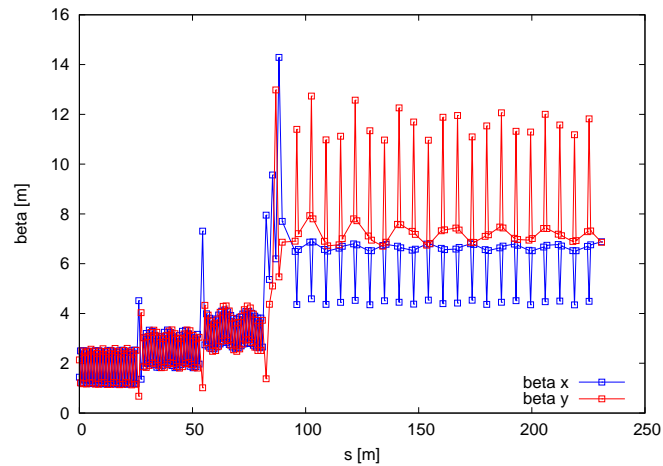


Figure 9: Betatron functions of the positron beam along the CLIC Injector Linac.

Figure 10 shows the transverse phase space distributions of the positrons at the end of the Injector Linac. The Twiss parameters and the rms normalized emittances derived from these two plots are in excellent agreement with those imposed by the design optics:

- $\epsilon_x^N = 9.27 \cdot 10^{-3}$  m.rad,  $\beta_x = 6.88$  m and  $\alpha_x = -0.38$ ,
- $\epsilon_y^N = 9.30 \cdot 10^{-3}$  m.rad,  $\beta_y = 6.86$  m and  $\alpha_y = -0.38$ .

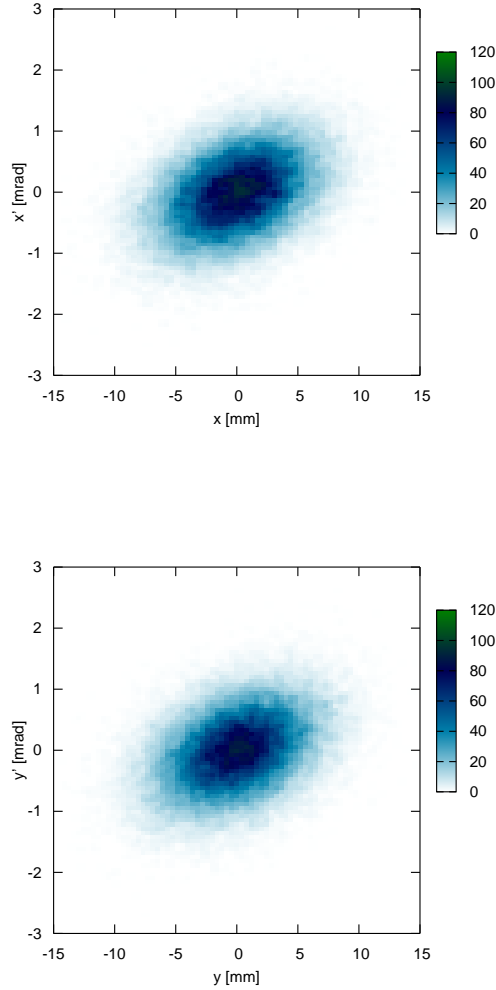


Figure 10: Transverse phase space distributions for the positrons at the end of the CLIC Injector Linac.

Figure 11 shows the longitudinal phase space distribution of the positrons at the end of the Injector Linac. The rms energy spread is 64.9 MeV, i.e. 2.7%, and the rms bunch length is 5 mm. Assuming a  $\pm 1\%$  energy acceptance for the pre-damping ring, then the fraction of positrons being actually injected and transported in this ring is 82%.

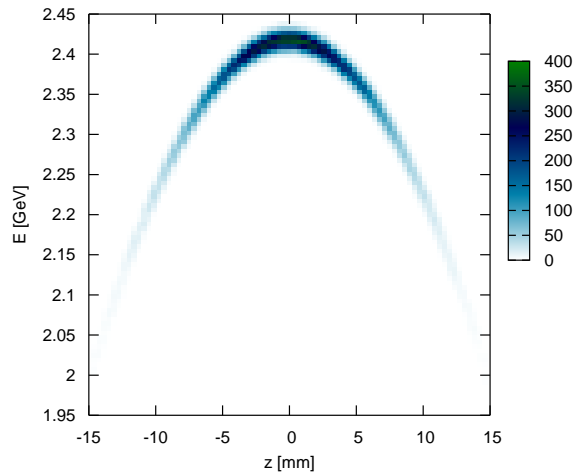


Figure 11: Longitudinal phase space distribution for the positrons at the end of the CLIC Injector Linac.

Figure 12 shows that the energy spread (at 2.42 GeV) can be brought below 1% with an initial rms bunch length of 2 mm instead of 5 mm (and an initial energy spread of 17.5 MeV instead of 7 MeV in order to keep the longitudinal emittance constant at the entrance of the Injector Linac). The possibility to implement a bunch compressor at the beginning of the Injector Linac was indeed already mentioned in [6]. Here, for every value of the initial bunch length used in PLACET, an optimization of the matching section is performed, in order to set the Twiss parameters to their design values at the entrance of the 16th accelerating structure and to minimize the emittance growth along the linac.

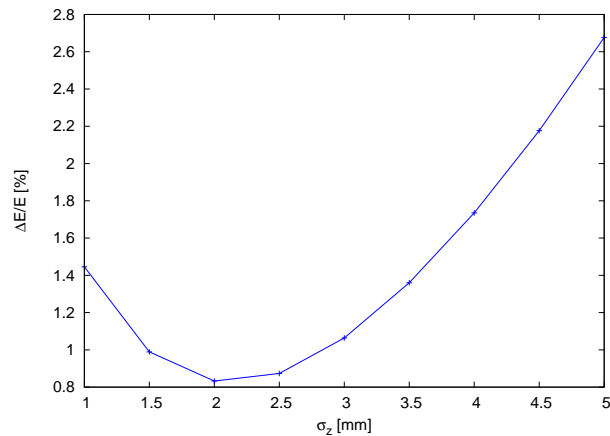


Figure 12: Energy spread for the positrons at the end of the CLIC Injector Linac, as a function of their initial rms bunch length.

A tracking study of the electrons along the Injector Linac was performed in [6], showing no significant emittance growth, and it is therefore not repeated here. Note that the  $e^-$  beam characteristics are much relaxed than for the  $e^+$  beam.

### 3 Design study of the CLIC Booster Linac

Downstream of the damping rings, the CLIC Booster Linac alternately accelerates the electron and positron main beams, from 2.42 to 9 GeV. The main beam properties at the entrance of the Booster Linac are given in Table 5.

Table 5: Beam characteristics at the entrance of the Booster Linac [1].

Beam energy	2.42 GeV
Normalized emittance $\gamma\epsilon_x$	$380 \cdot 10^{-9}$ m.rad
Normalized emittance $\gamma\epsilon_y$	$4.1 \cdot 10^{-9}$ m.rad
Energy spread $\sigma_E$	29 MeV
Bunch length $\sigma_l$	0.175 mm
Bunch charge $Q$	0.7 nC

In the CLIC Booster Linac, 73 accelerating structures operating at 4 GHz are used. Their length and loaded gradient are 3 m and 30 MV/m, respectively. A succession of triplets and accelerating structures is used all along the linac. Each quadrupole has a length of 36 cm and the spacing between two consecutive quadrupoles (as well as between the edge of an accelerating structure and a quadrupole) is 60 cm. With  $K_e = +0.189 \text{ m}^{-2}$  for the outermost quadrupoles of the triplet and  $K_m = -0.376 \text{ m}^{-2}$  for the quadrupole in the middle, both the horizontal and vertical betatron functions are equal to 30 m at the waist, located at the centre of the accelerating structure. In the middle of the second quadrupole (and of the periodic cell),  $\beta_x$  and  $\beta_y$  are respectively 27.2 and 33.6 m, see Figure 13.

Particle tracking studies with PLACET suggest that there is practically no emittance growth along the Booster Linac, assuming only short-range wakefields. Figure 14 shows the transverse phase space distributions obtained at the exit of the linac. The Twiss parameters and the rms normalized emittances derived from these two plots are:

- $\epsilon_x^N = 380 \cdot 10^{-9}$  m.rad,  $\beta_x = 104$  m and  $\alpha_x = -0.11$ ,
- $\epsilon_y^N = 4.1 \cdot 10^{-9}$  m.rad,  $\beta_y = 118$  m and  $\alpha_y = -0.10$ .

Figure 15 shows the longitudinal phase space distribution of the positrons at the end of the Booster Linac. There, the rms energy spread is 29 MeV, i.e. 0.32%, and the rms bunch length is 0.173 mm.

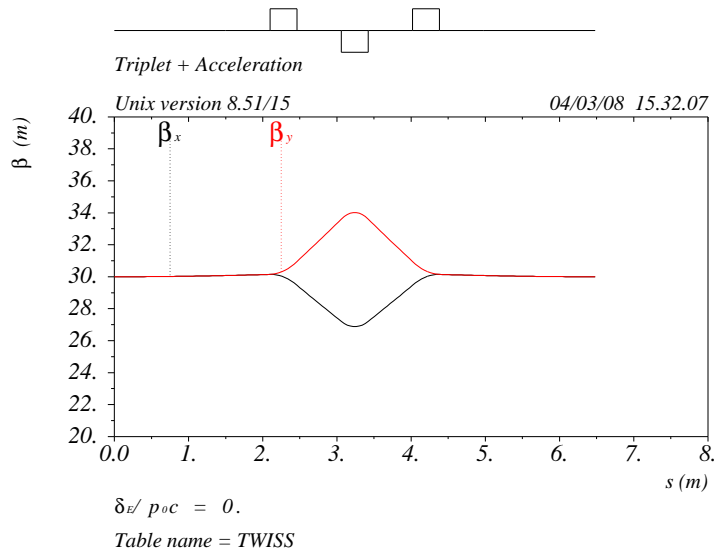


Figure 13: Betatron functions in a periodic cell of the CLIC Booster Linac.

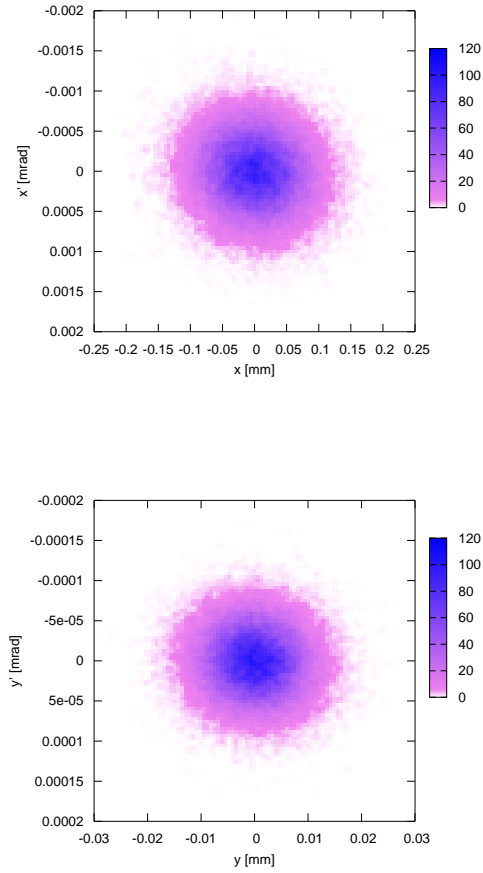


Figure 14: Transverse phase space distributions at the end of the CLIC Booster Linac.

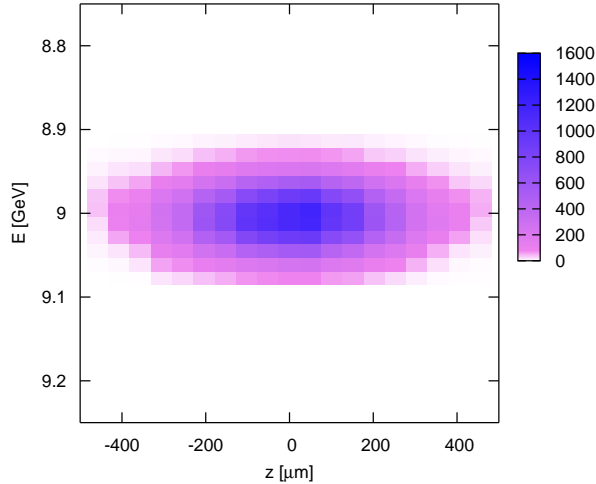


Figure 15: Longitudinal phase space distribution at the end of the CLIC Booster Linac.

## 4 Conclusion

Using the new CLIC parameters (October 2007), new optics have been designed for the Injector Linac and the Booster Linac of the CLIC Main Injector complex. The results of MAD simulations show that the optics for both linacs can be implemented with standard components (quadrupoles and accelerating cavities). The filling factor (i.e. the spacing between the components) is large enough to implement orbit correctors and beam instrumentation. The results of PLACET simulations show that short range wake fields have no effect on the beam performance for both linacs. The emittance growths are negligible and the beam transport efficiency is close to 100%. A road-map for future activities should include the following studies:

- the effects of the misalignments of the accelerating structures and the magnets.
- the effects of the long range wake fields, in particular in the Booster Linac where the emittances are very small. The vertical emittance, which is a critical parameter for the CLIC luminosity, should remain very close to 4 nm.rad.

## Acknowledgements

The authors wish to thank S. Döbert for fruitful discussions on accelerating structure design.

## References

- [1] L. Rinolfi, "CLIC Injector Complex Review and Status", presented at the CLIC'07 workshop, <http://project-clic07-workshop.web.cern.ch>
- [2] A. Ferrari, L. Rinolfi and F. Tecker, "Design study of the CLIC main beam Injector Linac", CLIC note 626.
- [3] A. Ferrari, L. Rinolfi and F. Tecker, "Particle tracking in the CLIC main beam Injector Linac", CLIC note 655.
- [4] <http://mad.home.cern.ch/mad/mad8web/mad8.html>
- [5] <http://savannah.cern.ch/project/placet>
- [6] A. Ferrari, A. Latina, L. Rinolfi and F. Tecker, "Beam dynamics studies in the CLIC Injector Linac", CLIC note 723; proceedings of PAC07, Albuquerque, New Mexico, USA.